Dependence of electrorheological response on conductivity and polarization time

M. Whittle, W. A. Bullough,* D. J. Peel, and R. Firoozian

Department of Mechanical and Process Engineering, The University of Sheffield, P.O. Box 600, Sheffield S1 4DU, United Kingdom
(Received 24 August 1993; revised manuscript received 5 January 1994)

The mechanisms which govern the performance of electrorheological (ER) fluids must be established if the response times and electrostress levels required for industrial applications are to be achieved. Earlier work by this group has led to a comprehensive description of the electrical and pressure response observed in engineering scale ER valve systems operating under realistic conditions. The present paper carries this program further by showing that in this regime the measured ER valve characteristics are consistent with the polarization-conductance mechanism commonly taken to be the basis for the generation of electrostress. Theoretical descriptions of ER fluids often ignore the role of conductance and frequency dependence of the permittivity. Here, within the context of a model incorporating these material properties and a polarization time, we examine factors affecting the speed, form, and magnitude of ER response. Using this model we are able to establish a relationship between the experimentally observed pressure and current for biased sine and step voltage excitation.

PACS number(s): 83.80.Gv, 47.50.+d

I. INTRODUCTION

Electrorheological (ER) fluids respond to large electric fields ($\sim 10^6$ V m^{-1}) with a substantial reversible change in rheological properties. Under zero-field conditions these fluids are generally characterized by simple Newtonian viscosity η, while at high fields they approximate a Bingham plastic and exhibit a yield stress S_0:

$$S = S_0 + \eta\dot{\gamma} \, , \tag{1}$$

where S is the total stress, and $\dot{\gamma}$ the strain rate. The ER response can occur in much less than a millisecond, and fast ER clutch and valve systems are currently under development with the aim of extending the range of flexible machine duties covered by electromagnetic mechanisms in some areas of operation [1–4]. To optimize such devices there is consequently considerable interest in reducing the response time and increasing the yield strength of the fluids on which many ER devices depend. The controllability of ER devices also depends upon an appreciation of these characteristics.

Particle polarization is now widely thought to be responsible for the interaction forces that lead to the rheological changes [5], and the ER fluids currently available are dispersions formed from polarizible particles supported by an insulating nonpolar fluid phase. A variety of materials has been used to make ER fluids, and the polarization mechanism seems not to be critical. Many ER fluids are "activated" by a small amount of water associated with the particles, and polarization by charge separation in an electrical double layer is the favored process. However, polarization may be achieved by electron transport if the particles are composed of a dry semiconducting material.

Associated with the rheological response of the fluid, structural changes occur that are commonly described as chaining or fibrillation. This alludes to the particle chains or columns that are seen to appear in dilute systems under zero or near-zero flow conditions. Computer simulations [6] suggest that under the conditions of flow, where the fluids are most likely to be of engineering use, the structure is characterized by the formation of sheets in the plane defined by the flow direction and the field. Within these sheets particle chains may form, but their length and lifetime are limited by the balance of viscous and electrical forces. In the absence of a field the same simulations suggest that particles align in the direction of the flow to form a so-called hexagonal string phase [6,7]. An increase in the interparticle force in response to the electric field is the primary cause of rheological changes, but under practical operating conditions the rate of transition between these two dynamic structures may be expected to influence the observed response time.

In a series of earlier papers [8–11] we analyzed the results from controlled tests on a set of five ER valve restrictors of different dimensions over a range of flow rates and voltage inputs operating at a well-controlled temperature. The valves consist of concentric cylinders of sufficiently large radii that they can be treated as a pair of flat plates (Fig. 1). Fluid flows along the length of the cylinders, and when a high voltage is applied rheological changes in the ER fluid lead to an increase in the pressure required to maintain the flow. The tests involved simultaneous recording of the pressure and current responses to step voltage and biased sine wave inputs as well as steady-state measurements. Because of the equipment limitations the sine wave tests were only made up to 200 Hz. All our results were carried out at 30 °C using a fluid containing 30% lithium polymethacrylate (Lipol) in a chlorinated hydrocarbon oil obtained from Laser Engineering Ltd., London. The polymer particles were "activated" with a water content of about 15%.

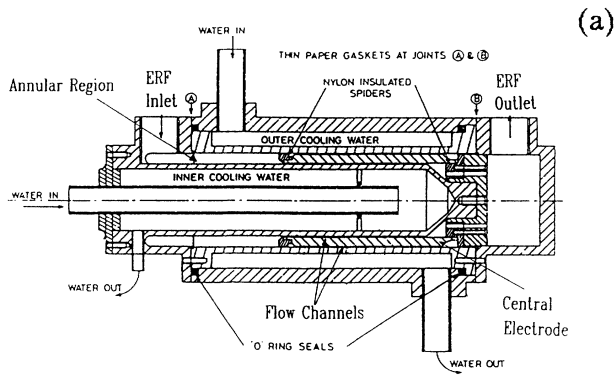Our earlier analysis of the current response has led to

---

*Fax: (0742) 753671.

FIG. 1. (a) Twin channel cooled experimental valve. (b) Simplified valve geometry used in the calculations. The ER fluid flows at a mean velocity U between plates of length l, width b, and gap h held at voltage V.

an electrical model for the valve which is of practical use to control engineers [8]. For small voltage changes on a steady background bias voltage we found that the valves have electrical characteristics described by the circuit of Fig. 2. However, as we discuss in more detail in Sec. III larger voltage changes invoke the nonlinear nature of the ER conductivity, and the model requires some modification. In addition, there is a small coupling effect between the pressure and current, apparently mediated by transient flow-rate changes, that is described in our earlier work [9]. Analysis of the valve pressure response has shown that traveling waves in the associated pipe-
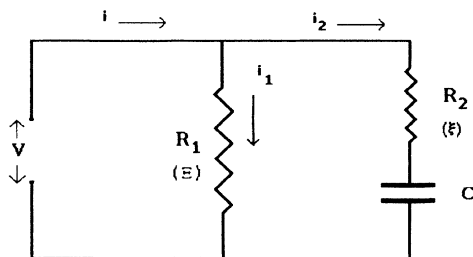

FIG. 2. Equivalent electrical circuit for the valve system. In the nonlinear analysis, resistance R_1 is replaced by a nonlinear conductivity coefficient Ξ, and resistance R_2 is replaced by ξ (see Sec. III).

work are probably responsible for the oscillatory features observed [11]. By removing these contributions we have been able to suggest a form of pressure response that would occur in the absence of these effects and thus isolate the underlying stress response of the ER fluid itself.

The present paper furthers this approach by showing that the underlying ER performance is consistent with the polarization-conductance mechanism commonly taken to be the basis for the generation of electrostress. We begin by outlining the relevant dielectric theory as a basis for the development of a model—Sec. II. In Sec. III we show that this model can account for the main features of the experimental electrical response. Finally, in Sec. IV we examine the consequences of this model for the interparticle force, the rheological response of the fluid, and thus the pressure response of the valve. The latter is compared with experimental data.

II. DIELECTRIC THEORY

For composite dielectric materials polarization occurs as a result of the mismatch of dielectric constants [12]. According to a simple point dipole model the dipole μ induced by an electric field E in a spherical particle (radius a) can be described in terms of the particle and fluid relative permittivities ε_p and ε_f:

$$\mu = 4\pi\varepsilon_0\varepsilon_f a^3 \beta E , \qquad (2)$$

where ε_0 is the permittivity of the free space. The factor β represents the dipolar distortion of the field surrounding the particle, and for a spherical particle takes the form

$$\beta = \frac{\varepsilon_p - \varepsilon_f}{\varepsilon_p + 2\varepsilon_f} . \qquad (3)$$

This factor is basic to ER theory. It arises from the constraint that the component of the electric displacement vector D, perpendicular to the particle surface, must be continuous at the boundary on passing from one dielectric medium to another. The dipole-dipole interaction potential between two such particles (separation r), aligned at an angle θ to the field, may be written

$$\Phi_{\mu\mu} = -\frac{\mu^2}{4\pi\varepsilon_0\varepsilon_f r^3}(3\cos^2\theta - 1) , \qquad (4)$$

and the interaction force is obtained by differentiation. If we assume that the structure of a static ER fluid is dominated by chains aligned along the field direction, that the particles within chains are initially touching, and that interchain interaction is negligible, then an approximate expression for the yield stress S_0 is [6]

$$S_0 \sim \tfrac{9}{8}\phi\lambda(1+\chi)\varepsilon_0\varepsilon_f(\beta E)^2 , \qquad (5)$$

where ϕ is the particle volume fraction and λ is a geometric factor, numerically about 0.45, which determines the point on the stress to strain curve where chain breaking occurs. It is well known that the dipole-dipole interaction force is valid only for polarizable spheres separated by more than a diameter, and that for closer interactions the force is considerably higher [6,13–15]. In

Eq. (5) this deficiency is addressed in an *ad hoc* manner by the factor χ which represents the extra force at particle contact compared to the point dipole model. Comparison of experimental yield stresses with Eq. (5) suggests that this factor may be as high as 200, while for the pure dipole-dipole interaction it vanishes. In deriving this expression it is notable that the dependence of force on particle size is balanced by the opposite dependence of chain density, with the result that the electrostress is independent of particle diameter. This is strictly true only for the relatively large particles ($> 10^{-6}$ m) currently used to manufacture ER fluids. For smaller particles Brownian motion can disrupt the structure on relatively short time scales, and should be considered [16]. Expressions containing β have commonly been used in representations of the interaction forces and stresses appearing in ER fluids. However, the frequency dependence and complex nature of β have usually been neglected. This may be a gross oversimplification, especially at low frequency, if a measurable conductivity is present in either particles or fluid [17].

The relative permittivity represents the polarization response of a material to an electric field, and is in general a frequency-dependent complex variable $\varepsilon^*(\omega)$ indicated by the asterisk:

$$\varepsilon^*(\omega) = \varepsilon'(\omega) - j\varepsilon''(\omega) , \tag{6}$$

where we have adopted the normal sign convention [18]. An equivalent representation can be made in terms of the complex conductivity $\sigma^*(\omega)$

$$\sigma^*(\omega) = \sigma'(\omega) + j\sigma''(\omega) , \tag{7}$$

and in general the representations are related by

$$\sigma^*(\omega) = j\omega\varepsilon_0\varepsilon^*(\omega) . \tag{8}$$

The polarization of a material may proceed on several time scales according to the contributing physical processes. These may include a high-frequency component related to fast electronic processes often termed the optical polarization since it can be related to the refractive index. Other processes, e.g., particle reorientation and ion transport, may contribute to the polarization at lower frequencies. Debye originally introduced an expression with a single relaxation time τ to account for reorientation resonances [19]:

$$\varepsilon^*(\omega) = \frac{\varepsilon_s - \varepsilon_\infty}{1 + j\omega\tau} + \varepsilon_\infty , \tag{9}$$

where ε_s is the static dielectric constant and ε_∞ is the high-frequency (optical) limit. In fact, this expression has much wider application than its original derivation would suggest [18]. The imaginary part of the permittivity

$\varepsilon''(\omega)$ represents the transient current that is drawn when a capacitor filled with that material is charged. Real dielectric materials may also have an appreciable dc conductivity which can be included in this formalism as an additional imaginary component:

$$\varepsilon^*(\omega) = \varepsilon' - j\left[\varepsilon'' + \frac{\sigma_s}{\omega\varepsilon_0}\right] , \tag{10}$$

where σ_s is the zero-frequency conductivity. Including the relaxation term of Eq. (9) explicitly, we have

$$\varepsilon^*(\omega) = \frac{\sigma_s}{j\omega\varepsilon_0} + \frac{\varepsilon_D}{1 + j\omega\tau} + \varepsilon_\infty , \tag{11}$$

where $\varepsilon_D = \varepsilon_s - \varepsilon_\infty$. Applying Eq. (8) to (11) we can obtain an equivalent expression for the frequency-dependent conductivity:

$$\sigma^*(\omega) = \sigma_s + \frac{j\omega\varepsilon_0\varepsilon_D}{1 + j\omega\tau} + j\omega\varepsilon_0\varepsilon_\infty . \tag{12}$$

We will use Eqs. (11) and (12) to model the dielectric behavior of the materials composing ER fluids.

III. CURRENT RESPONSE

A. Experimental results

The operation of devices using ER fluids requires large electric fields of the order $MV\,m^{-1}$. Our studies of ER valves [8] have shown that the steady-state current density i drawn at field E is given by

$$i = \Xi(E - E_T)^2 , \quad E > E_T , \quad i = 0 , \quad E < E_T , \tag{13}$$

where Ξ is a nonlinear conductivity parameter independent of valve dimension with units $A\,V^{-2}$, and E_T is a threshold field strength that depends on the flow rate. The combined results for all valves [8] gave a roughly linear dependence:

$$E_T = E_0 + BU , \tag{14}$$

with $E_0 \sim 0.1\ MV\,m^{-1}$, $B \sim 0.4\ MV\,m^2$ s, and U is the mean flow velocity through the valve in ms^{-1}. For a large step in the field (1–$4\ MV\,m^{-1}$), which typically occurs when a valve is activated, the resistors R_1 and R_2 in the electrical model shown in Fig. 2 must be replaced with nonlinear elements Ξ and ξ following Eq. (13). The current in the resulting circuit can be solved [8] to give a good representation of the current response $i_H(t)$, to a step in the field strength represented by the Heaviside function $H(0)$: $H(t - t') = 0$ for $t < t'$ and 1 for $t > t'$:

$$i_H(t) = (E - E_T)^2\left[[\Xi - \Xi_{st}\exp(-t/\tau_{st})] + \frac{\xi(\varepsilon_0\varepsilon_m)^2}{[\xi(E - E_T)t + \varepsilon_0\varepsilon_m]^2}\right]H(0) , \quad E > E_T \tag{15}$$

where Ξ determines the limiting steady-state current, ξ is related to the maximum current drawn in the initial response and is defined analogous to Ξ, and ε_m is the effective relative permittivity of the fluid mixture. In terms of the circuit in Fig. 2, this is related to the capacitance C (which, within the accuracy of the determination [8], is almost invariant with field) by a scale factor obtained by treating the valve as a parallel plate capacitor with gap h and surface area A:

$$\varepsilon_0 \varepsilon_m = C \frac{h}{A} \ . \tag{16}$$

We quote values of ε_m obtained in this way from our results [8] in Table I. Equation (15) also includes a relaxing term to account for the long-time drift in current probably associated with dynamic structural relaxation. The "structural" time constant τ_{st} is between 3 and 10 ms, and is associated with the parameter Ξ_{st} defined in an analogous way to Ξ. Equation (15) gives an excellent description of the observed response, although in practice a further adjustment must be made to include coupling with the mechanical response of the system thought to be related to the flow rate [9].

For small field steps ΔE imposed on a steady system at field E, the current response can be approximated by a linearized form:

$$\Delta i(t,E) = 2\Delta E (E - E_T)[\Xi - \Xi_{st}\exp(-t/\tau_{st})$$
$$+ \xi \exp(-t/\tau_1)]H(0) \ . \tag{17}$$

Neglecting the slowly relaxing "structural" term, Eq. (17) corresponds to the response of the linearized circuit in Fig. 2, and the time constant τ_1 represents the charging time for the capacitance C through the resistor r. In terms of the nonlinear conductive element ξ, this becomes

$$\tau_1 = \frac{\varepsilon_0 \varepsilon_m}{2\xi(E - E_T)} \ . \tag{18}$$

Mean response times obtained at two applied field strengths are given in Table I, and in Fig. 3 they are plotted to show the dependence on flow rate. The parameters ε_m and ξ may show some field dependence themselves, but any variation is lost in the experimental error of our determination.

Making the assumption that a large step response can be represented as a series of superimposed smaller steps, we find that the nonlinear response given in Eq. (15) can be represented reasonably well by a sum of linearized terms:
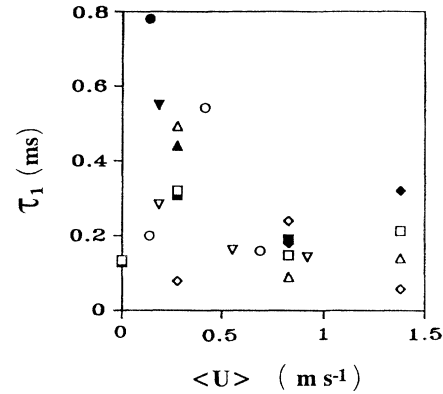

FIG. 3. The electrical relaxation time τ_1 plotted against the mean flow rate $\langle U \rangle$. $\square$, valve A. $\triangle$, valve B. $\circ$, valve C. $\Diamond$, valve D. ∇, valve E. Empty symbols: $E = 2.4$ MV m^{-1}; filled: $E = 1.2$ MV m^{-1}.

$$i_H(t) = \sum_{k=0}^{n} \Delta i(t, E_k) \ , \quad E_{k+1} = E_k + \Delta E \ , \quad E_0 = E_T \ . \tag{19}$$

A comparison between this summation representation, a single linear term, and the nonlinear response is shown in Fig. 4. In practice there is little change in the summation results for $n > 10$. This procedure is not strictly valid for a nonlinear system; nevertheless, it does give moderate improvement over the use of a single response time and is retained in the interests of generality and in recognition of the nonlinearity that appears under the operating conditions for which our results have been obtained. It enables us to represent the nonlinear response approximately as a sum of linear terms with a range of time constants determined by Eq. (18). Other methods of obtaining the distribution of time constants for related models are discussed by Daniel [18].

If $g(t)$ is the response of a system to a step function, we can obtain the response to a unit impulse by differentiation and then obtain the frequency response by one-sided Fourier transform [20]:

$$g^*(\omega) = \int_0^\infty \frac{d}{dt} g(t) e^{-j\omega t} dt \ . \tag{20}$$

Equation (17) can be transformed to the frequency domain to give an expression for the frequency-dependent conductance at field E, and since the conductivity $\sigma(t,E) = \Delta i / \Delta E$ we obtain

TABLE I. Experimental values obtained for electrical parameters (Ref. [9]). ε_p (eff) is obtained from Eq. (24).

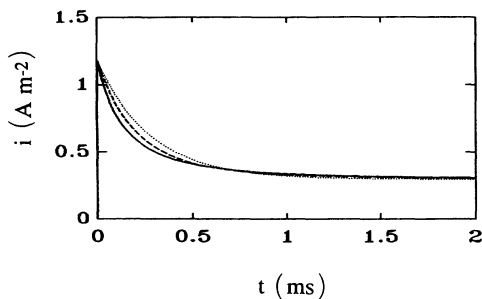| E (MV m^{-1})	ε_m (Expt.)	ε_p (eff)	σ_m (Ω^{-1}m^{-1})	ξ (mA MV^{-2})	σ_1 (Ω^{-1}m^{-1})	τ_1 (Expt.) (ms)
1.2	19.2±5.6	50.5±18.6	1.47×10^{-7}	291±114	6.4×10^{-7}	0.4±0.2
2.4	13.6±2.3	31.8±7.7	3.1×10^{-7}	202±115	9.3×10^{-7}	0.21±0.14

FIG. 4. Comparison of the nonlinear electrical model Eq. (15) —— with best-fit single relaxation time Eq. (17) · · · ·, and the summation approximation Eq. (19) — — — with $n = 20$ steps.

$$\sigma^*(\omega, E) = \sigma_m + \sigma_1 \frac{j\omega\tau_1}{(1+j\omega\tau_1)} - \sigma_{st} \frac{j\omega\tau_{st}}{(1+j\omega\tau_{st})} , \qquad (21)$$

where

$$\sigma_m = 2\Xi(E - E_T) , \quad \sigma_1 = 2\xi(E - E_T) ,$$
$$\sigma_{st} = 2\Xi_{st}(E - E_T) \qquad\qquad\qquad\qquad (22)$$

are field-dependent conductivities. The experimental time constant in Eq. (18) can now be written

$$\tau_1 = \frac{\varepsilon_0\varepsilon_m}{\sigma_1} . \qquad (23)$$

B. Theoretical current response

Many expressions have been derived for the dielectric constant and conductivity of heterogeneous mixtures in terms of particle and fluid parameters [21]. These expressions generally relate to randomly dispersed systems whose structure is not disturbed by the probe field. The situation for ER fluids is of course considerably complicated by the interaction of the field and structure. In the interests of mathematical simplicity, while retaining an element in the model to describe the principle, we adopt the simplest first-order approximation of a mixture model [22,23]:

$$\varepsilon_m = \phi\varepsilon_p + (1-\phi)\varepsilon_f , \qquad (24)$$

where ϕ is the volume fraction which for our experiments is 0.3. In fact this expression is appropriate for a capacitor whose plates are filled with fibers stretching from plate to plate [24] and may therefore be more appropriate to the case in hand than more complicated expressions. According to manufacturers' data the relative permittivity of the suspending fluid at 30 °C was 5.8. Combining this value with our experimental results for ε_m given in Table I, Eq. (24) gives an estimate of the particle static dielectric constant ε_p(eff) between 32 and 50.

The dielectric constant of water is 76.5 at 30 °C [24], and particles in our system have an absorbed water content of approximately 15%. Taking the dielectric constant of dry lithium polymethacrylate to be 3.5 [25], a straightforward linear sum gives a particle dielectric constant ε_p of about 14. This is a much smaller value than

our capacitance measurements would suggest, and may indicate the existence of alternative polarization mechanisms. In particular, the existence of lithium ions in and on the surface of the particles will lead to a charged double layer that can augment polarization [5,24]. However, we note that Marshall, Goodwin, and Zukoski [25] did not observe such a discrepancy when they made a similar calculation for their system. Furthermore, our valves were not calibrated as capacitance cells, and absolute values of the capacitance must therefore be regarded with some caution.

The experimental nonlinear parameter ξ is related to the maximum current drawn in the initial response, while the steady-state current is characterized by Ξ. The latter can be related to the steady-state mixture conductivity σ_m, which again we express in terms of the component conductivities by a mixture model

$$\sigma_m = \phi\sigma_p + (1-\phi)\sigma_f . \qquad (25)$$

For the series of valves studied [8,9] we obtained a value of $\Xi = 67$ mA MV^{-2}, giving values for σ_m at low and high fields (Table I). Since the base fluid conductivity is negligible [25] ($\sigma_f \sim 8 \times 10^{-10}$ Ω^{-1}m^{-1}), Eq. (25) then leads to an estimate of the particle conductivity σ_p (Table II). This turns out to be close to values of σ_1, and by analogy with Eq. (23) we might therefore write the particle polarization time as

$$\tau_p = \frac{\varepsilon_0\varepsilon_m}{\sigma_p} . \qquad (26)$$

This expression gives values within the experimental error of the average measured electrical response time τ_1 at each field strength (Table II). It must be said that the justification for the identification of σ_p with σ_1 is entirely empirical at this stage, and it would be interesting to see if it still applies at different volume fractions. Applying Eq. (11), for the particle permittivity we can now write

$$\varepsilon_p^*(\omega) = \frac{\sigma_p}{j\omega\varepsilon_0} + \frac{\varepsilon_p - \varepsilon_{p\infty}}{(1+j\omega\tau_p)} + \varepsilon_{p\infty} , \qquad (27)$$

where $\varepsilon_{p\infty}$ is the high-frequency limiting permittivity of the particle. For water [24], $\varepsilon_\infty \sim 4.5$, and for polymethacrylate we assume the static value of 3.5 holds, giving $\varepsilon_{p\infty} \sim 4.2$ by a volume average calculation.

It is not appropriate to treat the base fluid in the same way as the dispersed phase, and in any case applying a similar expression would give very long polarization times due to the low fluid conductivity. We include only conductive processes, and assume a rapid polarization of the fluid by molecular mechanisms so that

TABLE II. Values obtained from Eqs. (25), (26), (34), and (37) with $\varepsilon_p = 14$, $\varepsilon_f = 5.8$, and $\phi = 0.3$.

E (MV m^{-1})	σ_p (Ω^{-1}m^{-1})	τ_p (ms)	τ_c (ms)	τ_{mw} (ms)	ε_s	ε_∞
1.2	4.9×10^{-7}	0.35	0.46	0.76	13.2	8.3
2.4	10.3×10^{-7}	0.12	0.22	0.36	13.2	8.3

$$\varepsilon_f^*(\omega) = \frac{\sigma_f}{j\omega\varepsilon_0} + \varepsilon_{f\infty} \ , \tag{28}$$

where $\varepsilon_{f\infty}$ is the high-frequency limiting permittivity of the base fluid, assumed equal to the static value.

By combining these expressions using Eq. (24), we propose, as a working hypothesis, that the dielectric frequency response can be described by

$$\varepsilon_m^*(\omega) = \phi\left[\frac{\sigma_p}{j\omega\varepsilon_0} + \frac{\varepsilon_p - \varepsilon_{p\infty}}{(1+j\omega\tau_p)} + \varepsilon_{p\infty}\right]$$
$$+ (1-\phi)\left[\frac{\sigma_f}{j\omega\varepsilon_0} + \varepsilon_{f\infty}\right] \ , \tag{29}$$

which, by Eq. (8), we can write as

$$\sigma_m^*(\omega) = [\phi\sigma_p + (1-\phi)\sigma_f] + \phi\frac{j\omega\varepsilon_0(\varepsilon_p - \varepsilon_{p\infty})}{(1+j\omega\tau_p)}$$
$$+ j\omega\varepsilon_0[\phi\varepsilon_{p\infty} + (1-\phi)\varepsilon_{f\infty}] \ . \tag{30}$$

Putting

$$\tau_p\sigma_{\text{pol}} = \phi\varepsilon_0(\varepsilon_p - \varepsilon_{p\infty}) \ , \tag{31}$$

where σ_{pol} is a conductivity associated with the dielectric polarization current

$$\sigma_m^*(\omega) = \sigma_m + \sigma_{\text{pol}}\frac{j\omega\tau_p}{(1+j\omega\tau_p)}$$
$$+ j\omega\varepsilon_0[\phi\varepsilon_{p\infty} + (1-\phi)\varepsilon_{f\infty}] \ . \tag{32}$$

We do not expect to be able to account for a structural relaxation term with this model, and if we identify σ_{pol} with σ_1, and τ_p with τ_1, then the first two terms of Eq. (32) are identical to the linearized form of the experimental frequency response Eq. (21). As we have seen, $\sigma_1 \sim \sigma_p$, and we can therefore replace σ_{pol} with σ_p, although whether this is generally true must wait for further experimental confirmation. Both the real and imaginary parts of $\sigma_m^*(\omega)$ are positive, giving a positive phase angle between the current and voltage. This is experimentally confirmed by steady-state-biased sine experiments which show that current leads the voltage over the frequency range studied (< 200 Hz).

Expressed in the time domain as the response to a step at $t = 0$, Eq. (32) then becomes

$$\sigma_m(t) = [\sigma_m + \sigma_p\exp(-t/\tau_p)]H(0)$$
$$+ \varepsilon_0[\phi\varepsilon_{p\infty} + (1-\phi)\varepsilon_{f\infty}]\delta(0) \ . \tag{33}$$

The high-frequency components $\varepsilon_{p\infty}$ and $\varepsilon_{f\infty}$ are expressed as a delta function $\delta(0)$ at zero time, and will not be recorded in our time domain experiment [18]. If we remember that the slow structural term is not included in Eq. (33), this expression can be compared with the linearized time domain response Eq. (17). Notably, the inclusion of the particle polarization term in Eq. (27) is necessary to explain the initial current response and the inclusion of a direct current term [17] as the only contribution to the imaginary part of the particle permittivity is insufficient.

Nevertheless, for a system which includes only dielectric and conductive terms, Anderson [17] describes the transition from capacitance- to conductance-dominated polarization regimes with a "crossover" time constant τ_c:

$$\tau_c = \varepsilon_0\frac{2\varepsilon_f + \varepsilon_p}{2\sigma_f + \sigma_p} \ . \tag{34}$$

Since σ_f is negligible, this expression is similar to Eq. (26), but replaces ε_m [Eq. (24)] with $2\varepsilon_f + \varepsilon_p$. With $\varepsilon_p = 14$ as calculated according to the particle-water content (see above), Eq. (34) gives times rather longer than τ_p that compare more favorably with our experimental times (Table II). However, if the particle relative permittivity is set to ε_p (eff), then values of τ_c are well in excess of our results.

In the Maxwell-Wagner polarization model, charge builds up at the particle-fluid interface as a result of dielectric and conductivity mismatch. This mechanism is often proposed to account for ER phenomena [26]. The relaxation equations for this process take the form of the Debye expression Eq. (9), with ε_s, ε_∞, and τ calculated according to the dielectric parameters [21,24]

$$\varepsilon_\infty = \varepsilon_f\frac{2\varepsilon_f + \varepsilon_p + 2\phi(\varepsilon_p - \varepsilon_f)}{2\varepsilon_f + \varepsilon_p - \phi(\varepsilon_p - \varepsilon_f)} \ , \tag{35}$$

$$\varepsilon_s = 3\phi\sigma_f\frac{(2\sigma_f + \sigma_p)(\varepsilon_p - \varepsilon_f) - (2\varepsilon_p + \varepsilon_f)(\sigma_p - \sigma_f)}{[2\sigma_f + \sigma_p - \phi(\sigma_p - \sigma_f)]^2}$$
$$+ \varepsilon_f\frac{2\sigma_f + \sigma_p + 2\phi(\sigma_p - \sigma_f)}{2\sigma_f + \sigma_p - \phi(\sigma_p - \sigma_f)} \ , \tag{36}$$

$$\tau_{\text{MW}} = \varepsilon_0\frac{2\varepsilon_f + \varepsilon_p - \phi(\varepsilon_p - \varepsilon_f)}{2\sigma_f + \sigma_p - \phi(\sigma_p - \sigma_f)} \ . \tag{37}$$

The Maxwell-Wagner relaxation times τ_{MW} calculated from this formula, using $\varepsilon_p = 14$ as estimated from the particle water content, are just outside the experimental error for τ_1 (Table II) and rather longer than τ_p and τ_c. For low volume fractions we note that the Maxwell-Wagner time is identical to the crossover time Eq. (34). Estimated values of ε_s are comparable to ε_m but do not reflect the field dependence. Also, despite the incorporation of nonzero values for σ_p and σ_f the Maxwell-Wagner model does not include the direct current term introduced in Eq. (10) and therefore predicts vanishing conductivity at zero frequency. This apparent contradictory result is a consequence of the Debye form [Eq. (9)] of the Maxwell-Wagner expression which has the transform Eq. (12) with $\sigma_s = 0$. Schwann et al. [27] have previously been unable to account for the low-frequency dielectric behavior in electrolyte dispersions of polystyrene spheres using the Maxwell-Wagner model. Schwarz [28] included an extra term derived from polarization of the counterion atmosphere to explain the results. In the ER system studied here there is clearly a direct current term present at long times (or low frequency), and this contribution increases quadratically with field [Eq. (13)]. The detailed mechanism of current conduction in ER fluids is not clear, but in view of the high volume fractions and

structural modifications that take place we may envisage that the counterion polarization introduced by Schwarz may form bridges between particles forming conduction pathways through the fluid.

To summarize, using expressions based on Eq. (11) to describe the particle and fluid relative permittivities, and combining them using a simple mixture model, we obtain the frequency and time domain representations Eqs. (32) and (33). These expressions contain terms that can be related to Eqs. (17) or (21) which directly describe the experimental response. The expressions for τ_p and τ_c give results which agree favorably with the experimental current response, while τ_{MW} is a little long. Finally, the Maxwell-Wagner model is unable to account adequately for the low-frequency behavior of the permittivity, at least partly because it does not include a dc conductivity component.

IV. THE RHEOLOGICAL RESPONSE

A. Experimental results

The operation of electrorheological devices can often be linked, through the Bingham expression Eq. (1), to the appearance of yield stress. For example, in ER valves the relation between the steady-state ER pressure change ΔP_e and the yield stress is well known [29], and can be approximated by the linear expression

$$\frac{\Delta P_e}{l} = \frac{3S_0}{h} , \tag{38}$$

where l and h are the valve length and electrode gap. The yield stress S_0 appearing in this equation may be related to the dielectric mismatch factor β via Eq. (5). The latter was derived for a static ER fluid excited by an electric field prior to the imposition of a shear flow, and its application to a system flowing before the field is applied must be regarded with some caution. Equation (5) nevertheless suggests that there is a direct relation between the pressure appearing in an ER valve and the factor β which is in turn related directly to material properties. This relationship may be expected to extend to the frequency domain, although here other contributions must also be involved such as the time required for structural reorganization to take place.

We have previously described in detail some experimental results for the step voltage pressure response in an ER valve [10,11], and an example of the time domain step response is shown in Fig. 5. Using a multielement lumped parameter model we were able to show [11] that the oscillatory behavior between 2 and 6 ms originates from traveling elastic waves in the system pipework. This model included a hypothetical ER response of the form

$$S(t) = S_0 t \exp(-t/\tau) , \tag{39}$$

with a time constant $\tau \sim 0.35$ ms fitted on an empirical basis to account for the results. The model enables the prediction of the pressure response for an ER valve connected to the circulatory system by short pipes to minimize the interference from elastic waves, and the result is
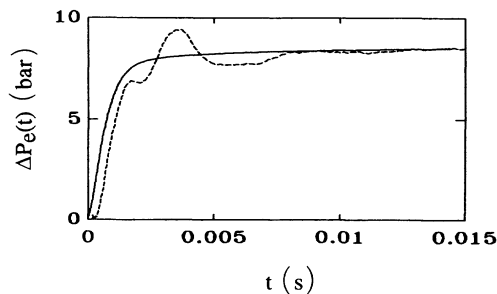
FIG. 5. The predicted time domain pressure response [11] for an ER valve in the absence of associated pipework ———. Compared with the experimental response – – –. Valve length, 0.1 m; width, 0.362 m; gap, 0.5 mm, flow rate, 9 L min^{-1} and $E = 2.4$ MV m^{-1}.

shown in Fig. 5. The initial delay seen in the experimental data can also be attributed to the system [11]. In Fig. 6 the experimental data are transformed using Eq. (20) to the frequency domain. This highlights the oscillatory contributions as peaks, and also compares the transformed response with data obtained directly in the frequency domain from steady-state-biased sine experiments. The biased sine voltage input here was relatively small (the sinusoidal field amplitude was typically ~ 0.1 MV m^{-1} on a dc bias of 2.4 MV m^{-1}), and the resulting output is in the linear-response regime.

B. Theoretical rheological response

In the static fluid, according to the model we are considering, the ER phenomenon is initiated by particle polarization which takes place on a time scale τ_p. It is a common observation that the faster the flow rate imposed the more rapidly ER devices can respond [1]. This suggests that for Couette flow we could write formally

$$S = f(E, \dot{\gamma}, \Delta t) , \tag{40}$$

where Δt indicates the time between switching on the electric and shear fields. Equivalently, we may say that S depends on the frequency of both field and mechanical oscillations. If we consider for the moment a hypotheti-
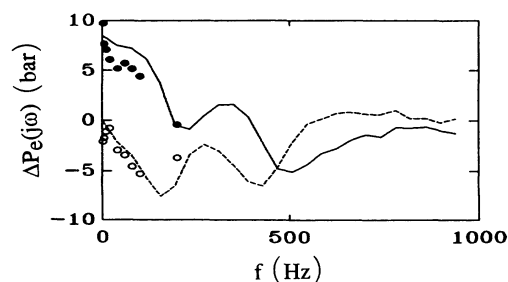
FIG. 6. Experimental step input pressure response (conditions as in Fig. 5) transformed to the frequency domain; real ——— and imaginary – – –. Compared with biased sine input results: real, ●; imaginary, ○.

cal system where polarization is instantaneous, there will be a corresponding change in the interaction force leading to some immediate change in the rheological properties of the fluid, which is not necessarily sufficient to manifest as a yield stress. This will be followed by further rheological changes as the particles take up positions of minimum energy. In a moving fluid this corresponds to a reorganization of the dynamic structure that may take place over several time scales [6], and is expected to be field and flow rate dependent. Even for the ideal case of instantaneous polarization the appearance of yield stress or the increase of effective viscosity is subject to a response time associated with structural reorganization. For the present case simulations suggest that structural time scales between 0.1 and 5 ms may be expected. Values of $\tau_{st} \sim (3-10$ ms$)$ are obtained in fitting the current response, and may correspond to relatively large scale cooperative changes. An attempt [11] to incorporate the notion of structural changes is embodied in Eq. (41), which for long time scales reduces to the Bingham constitutive equation [Eq. (1)]:

$$S(t) = S_0[1 - \exp(-K\dot{\gamma}t)] + \eta\dot{\gamma} . \tag{41}$$

In this expression, the yield stress changes smoothly from zero to S_0 as a function of the strain $\gamma = \dot{\gamma}t$ with a time constant $(K\dot{\gamma})^{-1}$. Equation (41) was designed to describe fluids excited in an initially static state when $K = S_0/G$, with G the shear modulus. In this case the formula expresses the idea that particle chains formed before any flow must be stretched under the strain γ before they break leading to yielding. The situation for a fluid which is already flowing before the electric field is applied is different. Nevertheless, to offer an explanation for the observed reduction in response time with flow rate, it is conceivable under these circumstances that particles are "helped" into dynamic equilibrium rather earlier by their motion in the velocity field. Such a mechanism might also be represented by Eq. (41), although the value of K is likely to be different.

If the fluid is treated as a continuum, there is an additional viscoelastic response time which refers to the rate of change of the velocity profile across the valve as the fluid changes character. In the type of ER valve we are considering, a range of flow rates exists, and this analysis is complicated. However, simulations that we have carried out [11] for the valve system using Eq. (41) suggest that the overall contribution from this viscoelastic process is relatively fast at about 0.015 ms. These considerations suggest that the basic frequency response of the interaction force as determined from a polarization model should be combined with further response times related to particle movement and the viscoelastic response.

We turn now to the implications of a frequency-dependent permittivity on the rheological response. This appears through β^2 in Eq. (5). Following the prescription which proved successful in describing the current response, we introduce Eqs. (27) and (28) for the particle and fluid permittivities into Eq. (3):

$$\beta^*(\omega) = \frac{\varepsilon_p^*(\omega) - \varepsilon_f^*(\omega)}{\varepsilon_p^*(\omega) + 2\varepsilon_f^*(\omega)} . \tag{42}$$

A similar approach was taken some years ago by Furedi and Valentine [30] to account for pearl chain formation in related systems. They used a model similar to Anderson's [17] and did not incorporate a separate polarization time which, as we have seen, is necessary to account for the observed current response. In terms of the simple theory [6] described briefly in Sec. II, the shear modulus G_0 can be written

$$G_0 = \frac{dS}{d\gamma} = \tfrac{9}{4}\phi(1+\chi)\varepsilon_0\varepsilon_f(\beta E)^2 , \tag{43}$$

from which comparison with Eq. (5) gives $S_0 = (\lambda/2)G_0$. Substitution of Eq. (42) gives an electrical contribution to the complex shear modulus $G_E^*(j\omega)$ in terms of β^{*2} and thus the yield stress becomes a complex function. If the structural response is sufficiently fast, we may expect the total stress to be dominated by this electrical contribution, so that

$$S(t) = \frac{\lambda}{2}G_E(t) + \eta\dot{\gamma} . \tag{44}$$

The analytical expression for β^{*2} incorporating Eqs. (11) and (12) is unwieldy, and we resort to computing its frequency dependence, assuming through Eqs. (43) and (44) that it forms the basis for the rheological response. In Figs. 7(a) and 7(b) we examine the behavior of β^{*2} for a single polarization relaxation time τ_p, and compare the result with the responses obtained for the cases of a vanishing τ_p and for zero particle conductivity. In these figures we have neglected σ_f and used a rather low particle conductivity of $\sigma_p = 10^{-7}$ Ω^{-1} m^{-1} to highlight its effect on this frequency scale. We have also assumed here
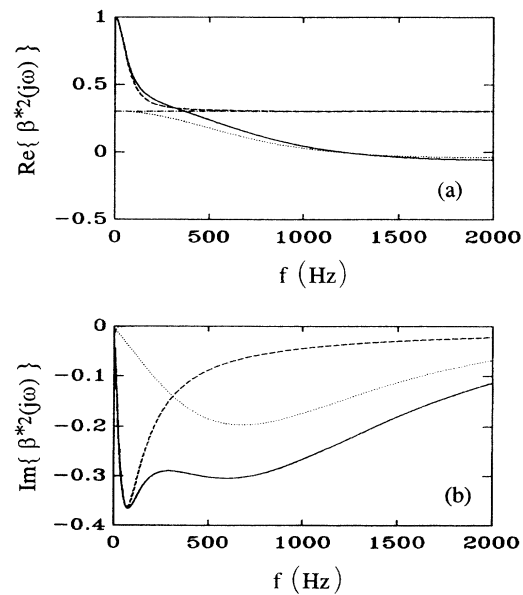
FIG. 7. (a) The frequency dependence of β^{*2} [Eq. (42)]: real components. $\varepsilon_p = 14$, $\varepsilon_{p\infty} = 3$, $\sigma_f = 0$, and $\varepsilon_{f\infty} = 3$. ——, $\sigma_p = 1 \times 10^{-7}$ Ω^{-1} m^{-1} and $\tau_p = 0.3$ ms. — — —, $\sigma_p = 1 \times 10^{-7}$ Ω^{-1} m^{-1}, and $\tau_p = 0$. $\cdots\cdots$, $\sigma_p = 0$ and $\tau_p = 0.3$ ms. — $\cdot$ — $\cdot$ —, $\sigma_p = 0$ and $\tau_p = 0$. (b) The frequency dependence of β^{*2} [Eq. (42)]: imaginary components. Conditions as in (a).

that the high-frequency limits $\varepsilon_{p\infty}$ and $\varepsilon_{f\infty}$ are equivalent and therefore cancel, thus ignoring any instantaneous response from this mechanism. The model commonly used to represent ER fluids is purely dielectric with instant polarization $(\sigma_p=0,\tau_p=0)$ and results in a flat frequency response for β^2 with magnitude of ~ 0.3 given by Eq. (3). With $\sigma_p=0$ and the inclusion of a polarization time τ_p, the same value of β^{*2} is attained only at low frequency. For nonzero σ_p with $\tau_p=0$, it can be seen that the effect of particle conductivity is to increase β^{*2} to unity at zero frequency which is significantly above the static dielectric expectations. The crossover relation from dielectric- to conductivity-dominated polarization [17] is evident at low frequency $\tau_c=0.885$ ms [see Eq. (34)]. In this case the finite limiting value at high frequency is the result of instantaneous polarization $(\tau_p=0)$ associated with ε_p, since the optical components have been chosen to cancel. If instead τ_p is chosen to be very long with nonzero σ_p, then the high-frequency contribution vanishes (not shown in the figure). The inclusion of the polarization term with an intermediate time constant τ_p comparable to τ_c further modifies the high-frequency response with attendant consequences for the short-time behavior. For this choice of parameters the resulting composite relaxation can evidently be resolved by eye into the crossover and polarization components. For the particle conductivities estimated for our system (Table II) the crossover and polarization times are closer and the components not so easily resolved.

For large voltage steps we found that an approximate model for the current response could be constructed by summing the linearized model over a series of smaller steps. In an attempt to get as close as possible to our experimental situation, we adopt the same approach here and calculate the frequency response of β^{*2} for a field step as a sum of linearized terms:

$$\beta^{*2}(\omega,E)= \sum_{k=0}^{n} \beta^{*2}(\omega,E_k,\Delta E) \ , \qquad (45)$$

where $\beta^{*2}(\omega,E_k,\Delta E)$ is calculated from Eq. (42) using Eqs. (27) and (28) with appropriate particle conductivities at field E_k estimated from Ξ on the basis of Eq. (22). The polarization time constants are calculated from the experimental relation Eq. (18), but Eq. (26) could be used with little error. The final result is shown in Fig. 8 and is not very different in shape to that obtained using a single conductivity and relaxation time from Table II. As we have already discussed, the crossover and polarization components cannot be resolved by eye.

If it is accepted that the peaks in the experimental spectrum are due to oscillations in the system pipework, then it can be seen that our present theoretical result is a reasonable form for the underlying rheological response, and correctly predicts the sign of the imaginary part which determines the direction of the phase shift. Steady-state-biased sine experiments have shown that the pressure lags the voltage while the current leads below 200 Hz. Our experimental work [11], described briefly in Sec. IV A, introduced a critically damped second-order response [Eq. (39)] as a model for the ER stress, which in
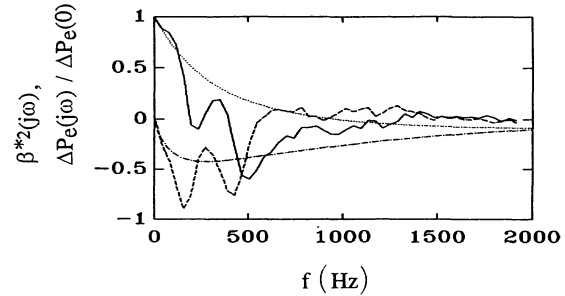

FIG. 8. The frequency dependence of β^{*2} obtained by the summation Eq. (45) with $n=20$ and $\tau_p=\tau_1=0.21$ ms, from Eq. (18). $\sigma_p=10.3\times10^{-7}$ $\Omega^{-1}m^{-1}$, $\varepsilon_p=14$, $\varepsilon_{p\infty}=4.2$, $\sigma_f=8\times10^{-10}$ $\Omega^{-1}m^{-1}$, and $\varepsilon_{f\infty}=7.3$; real $\cdots\cdots$ and imaginary $-\cdot-\cdot-\cdot$. Compared with the experimental normalized pressure response $\Delta P_e(j\omega)/\Delta P_e(0)$ (as in Fig. 6); real —— and imaginary $- - -$.

the frequency domain takes the form

$$T_n^*(j\omega)=\frac{1}{(1+j\omega\tau)^n} \ , \qquad (46)$$

with $n=2$. This function is shown in Fig. 9, where we compare normalized spectral densities (obtained by multiplying the complex spectrum by its conjugate) of the experimental pressure, the theoretical response, and a second-order response with $\tau=0.35$ ms. The low-frequency cusp in the experimental data is well represented by β^{*2}, but this feature cannot be reproduced by the second-order function. In the time domain this cusp corresponds to a slowly increasing component which has usually been attributed to slow structural behavior. The present model suggests that conduction processes may also contribute. We note that the real part of the theoretical response shown in Fig. 8 becomes negative beyond ~ 1000 Hz, which cannot be matched by a first-order function [$n=1$ in Eq. (46)].

To make a more direct comparison with our results, Fig. 10 shows the theoretical response function for β^{*2} transformed to the time domain by the inverse of Eq. (20), superimposed on the normalized pressure response for the appropriate field strength to which it is related through Eqs. (5) and (38). The low-frequency cusp in β^{*2} transforms to a slow upward drift which is reflected in
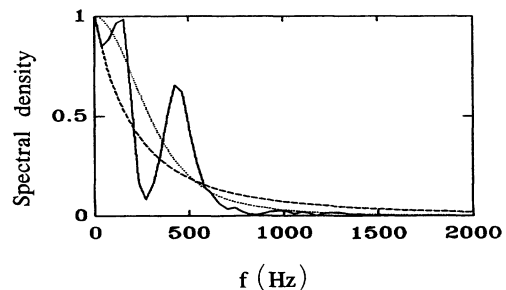

FIG. 9. Normalized spectral densities for the experimental pressure (as Fig. 6) $\Delta P_e(j\omega)$ ——, theoretical response β^{*2} $- - -$ as in Fig. 8, and $T_2(j\omega)$ [Eq. (46)] with $\tau=0.35$ ms $\cdots\cdots$.
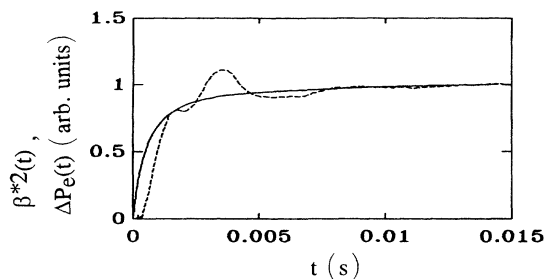
FIG. 10. Time domain response of β^{*2}——, obtained from the frequency response in Fig. 8 compared with the experimental pressure response (normalized to unity at $t = 1.5$ ms) to a step voltage input for an ER valve $---$. Conditions as in Fig. 5.

the experimental pressure. This figure should be compared with Fig. 5, which shows the expected pressure response with effects due to the system effectively removed. A good comparison is also obtained for lower values of the field strength, where the response time is somewhat slower.

Since we have used response times τ_1 based on electrical data to calculate β^{*2}, we have effectively linked the rheological and current responses via a polarization model. We argued earlier in this section that further response times related to initial particle movement and the viscoelasticity should be combined with the polarization response to give the final ER response. The comparison between the observed pressure and theoretical rheological response is so good that we are led to suggest that in this case such contributions are minimal. This concurs with a viscoelastic response time [11] of 0.015 ms obtained in simulations for our valve geometry, and according to Eq. (41) the presence of high shear rates (which may be up to 20 000 s^{-1} near the valve wall) in this system can lead to very rapid rheological changes once electric forces are established. Nevertheless, other slower structural processes

may be present that could modify the response on longer time scales.

V. CONCLUSIONS

We have used an electrorheological model involving the conductivity and a single polarization time associated with the particle to account for the experimental current and pressure responses in ER valve systems. We find that the inclusion of a polarization term is necessary to explain the observed current response. The Maxwell-Wagner model predicts response times rather longer than those observed in an experimental ER valve system, and it is unable to account for the low-frequency behavior of the permittivity. We have applied the same model to examine the consequences for the rheological response. The inclusion of a conductivity term increases the theoretical maximum possible yield stress compared to static dielectric models by a factor of at least 2, and also introduces a frequency dependence. The magnitude of the particle conductivity strongly influences the expected response time in the fluid mechanical properties. The inclusion of a relaxation time for polarization further modifies this response at high frequency and short times. The analysis involves neglecting the slow (probably structural) relaxation seen experimentally, but it shows in principle the link between the electrical and mechanical responses.

This model can form the basis for more comprehensive simulations of ER fluids in the future, leading to a better understanding of the relations between fluid materials and ER response times. It requires validation with other experimental results and other fluids, but further study of this model may go some way toward explaining why the correlation between ER fluid activity and simple dielectric mismatch is rather poor [31].

ACKNOWLEDGMENT

[1] A. Hosseini-Sianaki, W. A. Bullough, R. Firoozian, J. Makin, and R. C. Tozer, in *Proceedings of the International Conference Electrorheological Fluids, Carbondale, Illinois,* edited by R. Tao (World Scientific, Singapore, 1992), pp. 219–235.

[2] W. A. Bullough *et al.*, Proc. Inst. Mech. Eng. **27**, 87 (1993).

[3] R. Firoozian, W. A. Bullough, and D. J. Peel, Am. Soc. Mech. Eng. Publ. DE **18-4**, 45 (1989).

[4] D. J. Peel, D. Brooks, and W. A. Bullough, in *Proceedings of the 9th Conference on Fluid Machinery,* edited by L. Kisbocskói and A. Szabó (GTE, Budapest, 1991).

[5] H. Block and J. P. Kelly, J. Phys. D **21**, 1661 (1988).

[6] M. Whittle, J. Non-Newtonian Fluid Mech. **37**, 233 (1990).

[7] D. M. Heyes, J. Non-Newtonian Fluid Mech. **27**, 47 (1988).

[8] M. Whittle, R. Firoozian, W. A. Bullough, and D. J. Peel, Int. J. Mod. Phys. B **6**, 2683 (1992).

[9] M. Whittle, R. Firoozian, W. A. Bullough, and D. J. Peel, in *Proceedings of the 4th International Conference Electrorheological Fluids, Felkirch, Austria,* edited by R. Tao (World Scientific, Singapore, in press).

[10] M. Whittle, R. Firoozian, D. J. Peel, and W. A. Bullough, J. Intell. Mater. Syst. Struct. **5**, 105 (1994).

[11] M. Whittle, R. Firoozian, W. A. Bullough, and D. J. Peel, J. Non-Newt. Fluid Mech. (to be published).

[12] C. J. F. Bottcher, *Theory of Electric Polarization* (Elsevier, Amsterdam, 1973).

[13] M. J. Chrzan and J. P. Coulter, in *Proceedings of the International Conference Electrorheological Fluids, Carbondale, Illinois* (World Scientific, Singapore, 1992), pp. 175–191.

[14] M. H. Davis, J. Mech. Appl. Math. **17**, 499 (1964).

[15] D. J. Klingenberg and C. F. Zukoski, Langmuir **6**, 15

(1990).

[16] R. Tao, J. T. Woestman, and N. K. Jaggi, Appl. Phys. Lett. **55**, 1844 (1989).

[17] R. A. Anderson, in *Proceedings of the International Conference Electrorheological Fluids, Carbondale, Illinois* (Ref. [1]), pp. 81–90.

[18] V. Daniel, *Dielectric Relaxation* (Academic, London, 1967).

[19] P. Debye, *Polar Molecules* (Chemical Catalog Company, New York, 1929).

[20] J. A. Aseltine, *Transform Method in Linear System Analysis* (McGraw-Hill, New York, 1958).

[21] L. K. H. van Beek, Prog. Diel. **7**, 69 (1967).

[22] L. E. Nielsen, *Predicting the Properties of Mixtures* (Dekker, New York, 1978).

[23] A. F. Sprecher, Jr, Y. Chen, Y. Choi, and H. Conrad, in *Proceedings of the International Conference Electrorheological Fluids, Carbondale, Illinois* (Ref. [1]), pp. 142–153.

[24] J. B. Hasted, *Aqueous Dielectrics* (Chapman and Hall, London, 1973).

[25] L. Marshall, C. F. Zukoski, and J. W. Goodwin, J. Chem. Soc. Faraday Trans. 1 **85**, 2785 (1989).

[26] K. D. Weiss and J. D. Carlson, in *Proceedings of the International Conference Electrorheological Fluids, Carbondale, Illinois* (Ref. [1]), pp. 264–279.

[27] H. P. Schwann, G. Schwarz, J. Maczuk, and H. Pauly, J. Phys. Chem. **66**, 2626 (1962).

[28] G. Schwarz, J. Phys. Chem. **66**, 2636 (1962).

[29] Zheng Lou, R. D. Ervin, and F. E. Filisko, in *Proceedings of the International Conference Electrorheological Fluids, Carbondale, Illinois* (Ref. [1]), pp. 398–423.

[30] A. A. Furedi and R. C. Valentine, Biochim. Biophys. Acta **56**, 33 (1962).

[31] L. F. Evans, I. Harness, P. E. Kermode, and J. E. Stangroom, in *Proceedings of the International Conference Electrorheological Fluids, Carbondale, Illinois* (Ref. [1]), pp. 154–166.